1982

Motion Analysis of Rolling Piston in Rotary Compressor

T. Yanagisawa

T. Shimizu

I. Chu

K. Ishijima

MOTION ANALYSIS OF ROLLING PISTON IN ROTARY COMPRESSOR

Tadashi Yanagisawa
Research Associate*
Itsuo Chu
Senior Engineer**

Takashi Shimizu
Professor*
Kouji Ishijima
Engineer**

* Department of Mechanical Engineering, Shizuoka University, Hamamatsu, Japan.
** Shizuoka Works, Mitsubishi Electric Corporation, Shizuoka, Japan.

ABSTRACT

This paper is concerned with rolling piston type rotary compressor for air conditioner. rotating motion of the rolling piston is theoretically analysed using mathematical model which consists of dynamic equation of rolling piston, equation of force equilibrium and equation of bearing characteristic. Also the motion in operating compressor is measured by detecting the change of electrostatic capacity between rolling piston face and electrode mounted on cylinder head surface. After signal analysis, it is proved that rolling piston is sliding positive and negative alternately on the vane tip and it is rotating forward slowly around its center. Theoretical results are in good agreement with experimental results and the validity of the model is verified.

INTRODUCTION

Rolling piston type rotary compressors are widely used for air conditioners. They have many advantages of small size, light weight, low cost and high performance as compared with reciprocating compressors. However, they also have disadvantages peculiar to the rotary compressors. One of these is friction loss which occurs closely related to motions of rolling piston (or roller) and vane (or blade) of the compressor.

In the past there have been some investigations to analyse motion of rolling piston and/or related friction loss [1-4]. However, most of them are analysing these by assuming steady state condition that rolling piston is rotating at average frequency and friction loss occurs under average loading. And the calculated results are not at all verified by experiment.

This paper attempts to analyse motion of rolling piston theoretically and experimentally. In theoretical analysis dynamic equation of rolling piston is solved with characteristic equations of finite length bearing. At experiment rotational motion of rolling piston in the operating compressor is measured using electrodes which detect electrostatic capacity. Theoretical results are verified by the comparison with experimental results.

THEORETICAL ANALYSIS

Dynamic Equation of Rolling Piston

Figure 1 shows schematic view of a rolling piston type rotary compressor. A rolling piston mounted on an eccentric of a shaft divides a cylinder room into two chambers, suction and compression chambers, associated with a vane. As the shaft rotates, the rolling piston rotates with the eccentric in the cylinder, which causes suction work in the suction chamber and compression and discharge work in the compression chamber.

There are many moments acting on the rolling piston. They are journal bearing moment M_c at the inner surface, vane tip moment $r \times F_t$ at the outer surface, oil film moment M_b at the end faces.

Usually at the nearest point (A in Fig.1) between outer surface of rolling piston and inner surface of cylinder, some clearance exists and such moment that affects motion of rolling piston doesn't occur. Therefore, Dynamic equation of rolling piston around its center is expressed as follows.

$$I_p \dot{\omega}_p = M_c - r F_t - M_b \qquad (1)$$

Each moment will be analysed in the following.

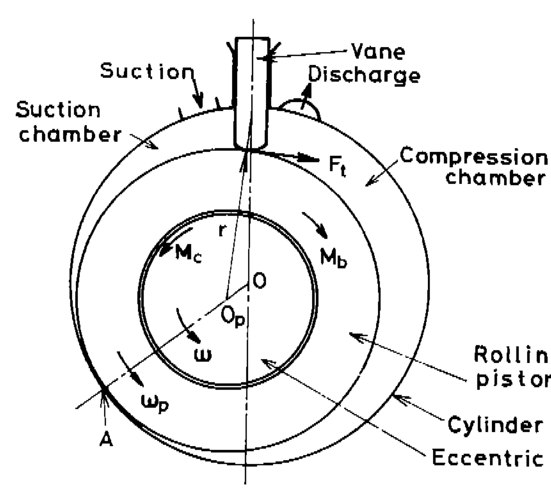

Fig. 1 Schematic view of rolling piston type rotary compressor

Analysis of Bearing Moment

The rolling piston and the eccentric constitute a kind of journal bearing. However, the rolling piston as bearing is rotating and bearing load is changing its magnitude and its direction. In this paper, the rolling piston bearing is analysed as an equivalent bearing shown in Fig. 2. Namely, the journal is rotating at the angular velocity of $(\omega-\omega_p)$ and the bearing is not rotating. And direction of bearing load F is changing at the angular velocity of $(\dot{\theta}_f-\omega_p)$. Then, bearing moment M_c is given by next equation.

$$M_c = \frac{2\pi\eta\,(\omega-\omega_p)\,\ell_c\,r_c^3}{c\sqrt{1-\varepsilon^2}} - \frac{1}{2}\,c\varepsilon F\sin\phi \tag{2}$$

Where, attitude ε and attitude angle ϕ of the bearing should be calculated based on theory of finite length bearing under dynamic loading. Here we use approximate calculating method developed by Nakagawa and Aoki [5,6]. According to that method, bearing pressure p is approximately expressed as follows.

$$\begin{aligned} p = \frac{24\eta}{\pi}\left(\frac{r_c}{c}\right)^2 \frac{\sin(\pi z/\ell_c)}{(1+\varepsilon\cos\psi)^2}\,[\{\omega+\omega_p - 2(\dot{\theta}_f+\dot{\phi})\} \\ \times(A_1\sin\psi - A_2\sin 2\psi + A_3\sin 3\psi) \\ + 2\dot{\varepsilon}\,(C_0 - C_1\cos\psi + C_2\cos 2\psi - C_3\cos 3\psi)] \end{aligned} \tag{3}$$

Where, A_1~A_3 and C_0~C_3 are constant and function of bearing length ratio to diameter [5].

Balancing equation of oil film pressure and bearing load F is put down as follows.

$$\left.\begin{aligned} F\sin\phi &= \int_0^{\ell_c}\int_{\psi_1}^{\psi_2} p r_c \sin\psi\, d\psi\, dz \\ F\cos\phi &= -\int_0^{\ell_c}\int_{\psi_1}^{\psi_2} p r_c \cos\psi\, d\psi\, dz \end{aligned}\right\} \tag{4}$$

Where ψ_1 and ψ_2 are boundary angles of positive pressure resion of oil film and they are the values of ψ which satisfy $p=0$ at Eq.(3). Using these values Eq.(4) is represented as follows.

$$\left.\begin{aligned} F\sin\phi &= A\{\Phi(A_1I_{11}+A_2I_{12}+A_3I_{13}) \\ &\quad +2\dot{\varepsilon}(C_1I_{21}+C_2I_{22}+C_3I_{23})\} \\ F\cos\phi &= A\{\Phi(A_1J_{11}+A_2J_{12}+A_3J_{13}) \\ &\quad +2\dot{\varepsilon}(C_1J_{21}+C_2J_{22}+C_3J_{23})\} \end{aligned}\right\} \tag{5}$$

Where, $A=\eta r_c \ell_c (r_c/c)^2/\pi$, $\Phi=\omega+\omega_p-2(\dot{\theta}_f+\dot{\phi})$ and I_{11}~I_{23}, J_{11}~J_{23} are functions of ε, ψ_1 and ψ_2 [5]. From Eq.(5) time differentials of attitude ε and attitude angle ϕ are given as follows.

$$\dot{\varepsilon} = \frac{F(B_1\cos\phi - B_3\sin\phi)}{2A(B_1B_4 - B_2B_3)} \tag{6}$$

$$\dot{\varepsilon} = \frac{1}{2}(\omega+\omega_p-2\dot{\theta}_f) - \frac{F(B_4\sin\phi - B_2\cos\phi)}{2A(B_1B_4 - B_2B_3)} \tag{7}$$

Where $B_1=A_1I_{11}+A_2I_{12}+A_3I_{13}$, $B_2=C_1I_{21}+C_2I_{22}+C_3I_{23}$,
$B_3=A_1J_{11}+A_2J_{12}+A_3J_{13}$, $B_4=C_1J_{21}+C_2J_{22}+C_3J_{23}$.

ε and ϕ are got by simultaneous integration of Eqs.(3), (6) and (7) numerically.

Analysis of Bearing Load

Figure 3 shows forces acting on the rolling piston, namely, gas compression force F_p, centrifugal force F_e, vane contact force F_n and F_t. Combined force of them becomes bearing load. Magnitude F and direction θ_f of bearing load are expressed as follows when F_r and F_θ are radial and angular components of bearing load given by Eqs.(10) and (11) respectively.

$$F = \sqrt{F_r^2 + F_\theta^2} \tag{8}$$

$$\theta_f = \theta + \mathrm{Tan}^{-1}(F_\theta/F_r) \tag{9}$$

$$F_r = F_p\cos\frac{\theta+\alpha}{2} - F_n\cos(\theta+\alpha) - F_t\sin(\theta+\alpha) + F_e \tag{10}$$

$$F_\theta = -F_p\sin\frac{\theta+\alpha}{2} + F_n\sin(\theta+\alpha) - F_t\cos(\theta+\alpha) \tag{11}$$

In above equations, centrifugal force F_e and gas compression force F_p are evaluated as follows.

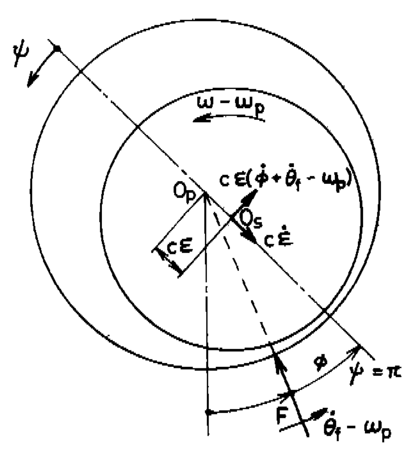

Fig. 2 Model of rolling piston bearing

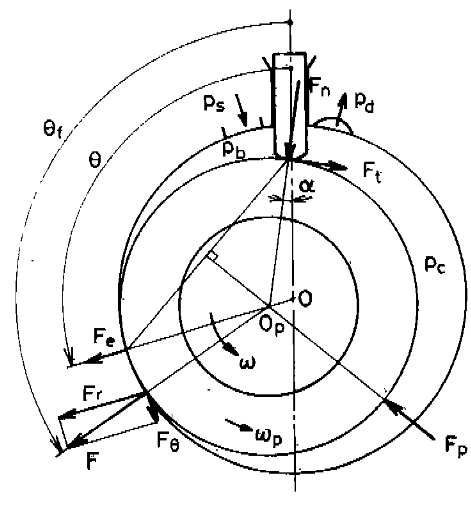

Fig. 3 Forces acting on rolling piston

$$F_e = m_p e\,\omega^2 \tag{12}$$

$$F_p = 2r\ell(p_c - p_b)\sin\frac{\theta+\alpha}{2} \tag{13}$$

Here, suction chamber pressure p_b is assumed to be constant and equal to suction pressure p_s of the compressor. And compression chamber pressure p_c is assumed to rise adiabatically till discharge valve opens (pressure p_d', angle θ_d) and after that to decrease linearly with shaft rotational angle θ as shown in Fig.4.

$$p_b = p_s \tag{14}$$

$$p_c = \begin{cases} p_s\,(V_s/V_c)^{\kappa} & (\theta \leqq \theta_d) \\ p_d + (p_d' - p_d)\dfrac{2\pi-\theta}{2\pi-\theta_d} & (\theta > \theta_d) \end{cases} \tag{15}$$

Where, V_s is suction volume and V_c is compression chamber volume expressed as follows.

$$V_s = \pi\,(R^2 - r^2)\,\ell + V_t \tag{16}$$

$$V_c = V_s - \frac{1}{2}R^2\ell\theta + \frac{1}{2}r^2\ell(\theta+\alpha) + \frac{1}{2}e\ell(r+r_v)\sin(\theta+\alpha) - \frac{1}{2}r_v^2\ell\tan\alpha - \frac{1}{2}b\ell x \tag{17}$$

Analysis of Forces acting on vane

Figure 5 shows forces acting on the vane, namely, contact forces F_t and F_n with rolling piston, contact forces R_1, R_2 and R_{t1}, R_{t2} with vane slot, pressure differential force F_h across the vane within the cylinder, pressure differential force F_d in and out of cylinder, vane spring force F_k and inertial force F_m. Each force is expressed as follows.

$$F_h = x\ell(p_c - p_b) \tag{18}$$

$$F_d = \ell b p_d - \ell p_c(b/2 + r_v\sin\alpha) - \ell p_b(b/2 - r_v\sin\alpha) \tag{19}$$

$$F_k = k(x_0 - x) \tag{20}$$

$$F_m = -m_v\ddot{x} \tag{21}$$

Here, balancing equations of acting forces and moments are expressed as follows.

$$F_h + R_2 - R_1 + F_t\cos\alpha - F_n\sin\alpha = 0 \tag{22}$$

$$F_d + F_h + F_m - R_{t1} - R_{t2} - F_t\sin\alpha - F_n\cos\alpha = 0 \tag{23}$$

$$R_2(a_1 - r_v + r_v\cos\alpha) - R_1(x - r_v + r_v\cos\alpha) + F_h(x/2 - r_v + r_v\cos\alpha) + b(R_{t2} - R_{t1})/2 - r_v\sin\alpha(F_t\sin\alpha + F_n\cos\alpha) = 0 \tag{24}$$

At contact points, acting forces are assumed to have next relations as μ_v is coefficient of friction at contact point with rolling piston and μ_s is coefficient of friction at contact point with vane slot.

$$F_t = \mu_v F_n \tag{25}$$

$$R_{t1} = \mu_s R_1\ ,\quad R_{t2} = \mu_s R_2 \tag{26}$$

From Eqs.(22) ~ (24), normal force F_n at vane tip is derived as follows.

$$F_n = \{(F_d + F_k + F_m)(x - a_1) + \mu_v F_h(a_1 + b\mu_s)\} / [(\cos\alpha + \mu_v\sin\alpha)(x - a_1 - 2\mu_s r_v\sin\alpha) + \mu_s(\sin\alpha - \mu_v\cos\alpha)\{x + a_1 + b\mu_s - 2r_v(1 - \cos\alpha)\}] \tag{27}$$

For μ_v and μ_s, experimental values will be used.

Oil Film Moment at Rolling Piston Faces

There exists oil film between rolling piston face and cylinder head surface. Its shearing force acts as braking moment on rotating rolling piston. By assuming, at each face, oil film thickness is equal to the half of total rolling piston face clearance δ_b. The moment M_b at both faces is expressed as follows.

$$M_b = 2\pi\eta\omega_p(r^4 - r_c^4)/\delta_b \tag{28}$$

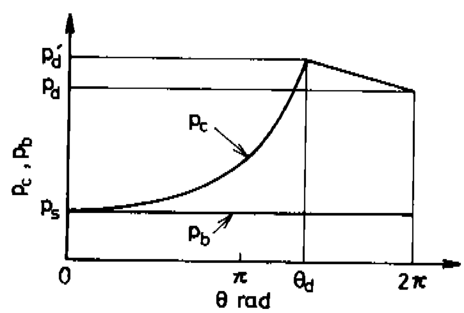

Fig. 4 Pressure - angle diagram

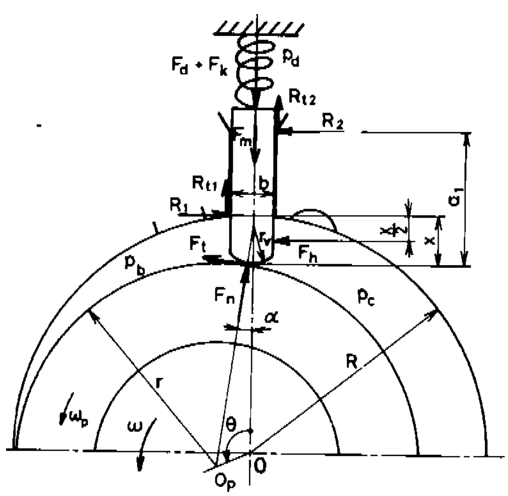

Fig. 5 Forces acting on vane

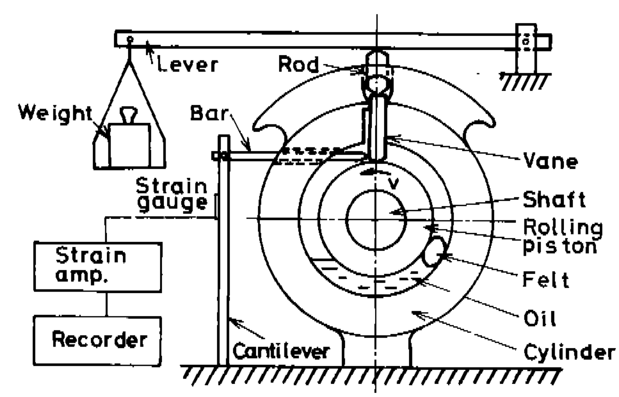

Fig. 6 Experimental apparatus to measure coefficient of friction at vane tip

EXPERIMENT

Measurement of Coefficient of Friction

Figure 6 shows experimental apparatus to measure coefficient of friction at contact point between vane tip and outer surface of rolling piston. Rolling piston is located at cylinder center and is rotating with shaft driven by a variable speed motor. While, vane is set in the vane slot loaded by the weight through lever and rod. Frictional force arisen at vane tip is transmitted to cantilever by the bar and measured by strain gauge on the cantilever. Lubricating condition is such that outer surface of rolling piston is wetted by the felt drenched with refrigerating oil. At experiment, loading weight and rotational frequency of rolling piston and temperature of lubricating oil are changed.

Figure 7 shows measuring apparatus of coefficient of friction at vane side. In the vane slot the vane is moving back and forth according to the oscillating motion of lever driven by cam shaft. While, horizontal force perpendicular to moving direction is loaded by spring balance. Frictional force between vane sides and vane slot is transmitted to lever through rod and measured by strain gauge on the lever. Lubricating condition is such that refrigerating oil is continuously poured from the top of the vane. At experiment, horizontal force and rotational frequency of cam shaft are changed.

Measurement of Rolling Piston Motion

Figure 8 shows a schematic view of an experimental compressor for measurement of rolling piston motion. Figure 9 shows cross section (A-A in Fig.8) of the compressor. On the rolling piston face, twelve small slot (1mm width × 1mm depth, $\pi/6$ rad pitch) are radially digged by electrical discharge machining. On the other hand, on the frame (upper cylinder head) surface, electrically insulated three electrodes (1 mm dia.) are located on the pitch circle which overlapps every slot and their pitch angle is one third of the slot pitch angle.

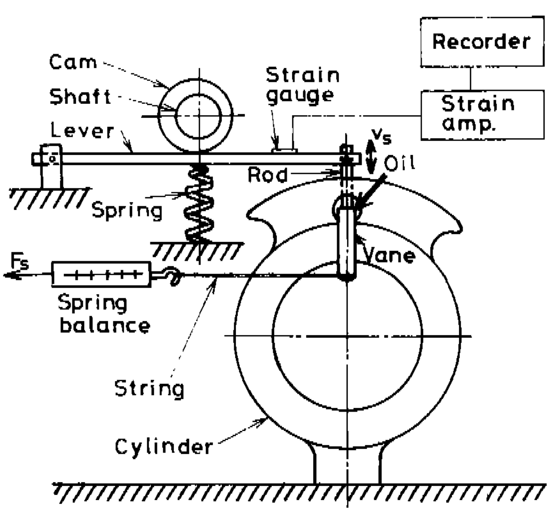

Fig. 7 Experimental apparatus to measure coefficient of friction at vane side

Rotating motion of rolling piston is catched by picking up the signals of electrostatic capacity between electrode and rolling piston face. By analysis of three signals from electrodes, not only average but also instantaneous rotation of rolling piston during one revolution of shaft become clear.

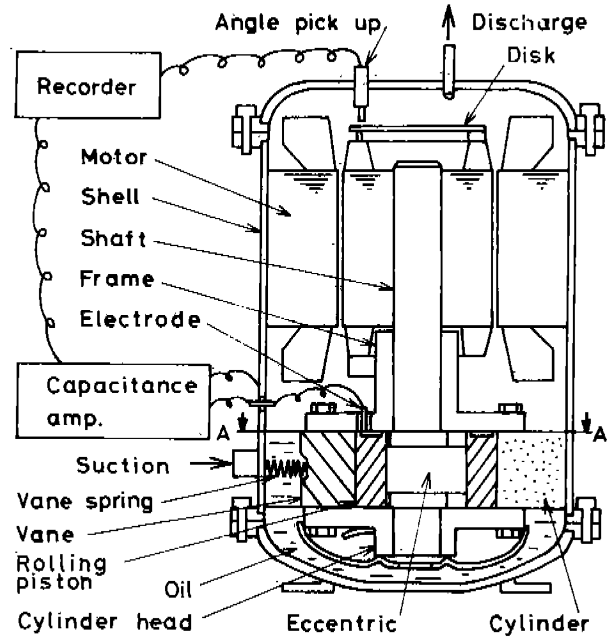

Fig. 8 Schematic view of experimental compressor

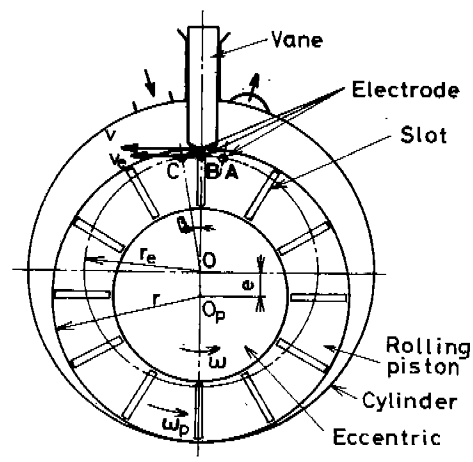

Fig. 9 Cross section (A-A in Fig.8) of the compressor

Table 1 Main dimensions of four designs of compressor used for experiment (dim. in mm)

Comp.	R	r	r_c	r_v	l	l_c	a	b
1	27.0	24.3	14.4	6.0	23.8	14.0	24.0	4.7
2	27.0	21.8	15.7	6.0	30.8	21.0	24.0	4.7
3	29.0	25.5	17.5	6.0	50.0	32.0	26.0	4.7
4	29.0	23.3	17.5	6.0	50.0	32.0	26.0	4.7

Rotational angle of the shaft is detected by the eddy current type transducer whish senses revolution of disk with teeth fixed on the motor rotor.

Experimental compressor is joined to refrigerating cycle used refrigerant R-22 as working fluid. The compressor is operated under given steady condition, and signals from rotating rolling piston and shaft are recorded by ultra-violet recorder. Table 1 shows main dimensions of four designs of compressor used for experiment.

By the way, in the case of compressors 2, 3 and 4 in Table 1, because of dimensional limitation, only average rotation of rolling piston is measured by using one electrode and one slot.

RESULTS AND DISCUSSIONS

Measured Results of coefficient of Friction

Figure 10 shows coefficient μ_v of friction at vane tip. μ_v is defined as F_t/F_n. Horizontal axis of the figure is expressed by dimensionless lubricating parameter $\eta v/(F_n/\ell)$. Not depending on experimental conditions, μ_v is almost constant in the range of $\eta v/(F_n/\ell)$ less than 10^{-6}, where lubricating condition is considered to be boundary condition. On the other hand, in the range of larger $\eta v/(F_n/\ell)$, μ_v is decreasing with increase of $\eta v/(F_n/\ell)$, this means mixed lubricating condition. In this paper μ_v is approximated by next empirical formula.

$$\eta_v = 0.15 - 35\sqrt{\eta v/(F_m/\ell)} \tag{29}$$

In addition, measured μ_v is not so much affected by the supplying condition of lubricating oil.

Figure 11 shows coefficient μ_s of friction at vane side. By assuming that μ_s at two contact points on both sides of vane are equal, μ_s is calculated by next equation.

$$\mu_s = \frac{R_{t1}}{R_1} = \frac{R_{t2}}{R_2} = \frac{R_{t1}+R_{t2}}{R_1+R_2} \tag{30}$$

Where, the denominator $R_1+R_2(\equiv R_{12})$ of the most right side of Eq.(30) is given by Eq.(31) taking account of moment balance of acting forces. While, the numerator $R_{t1}+R_{t2}$ is evaluated by Eq.(32) compensating inertial force F_m of the vane.

$$R_{12} = F_s(2\ell_2-\ell_1)/\ell_1 \tag{31}$$

$$R_{t1}+R_{t2} = F_\ell + F_m \tag{32}$$

In Fig.11, though μ_s is a little scattered, μ_s is considered to be constant in the wide range of dimensionless lubricating parameter $\eta v_s/(R_{12}/\ell)$. This means lubricating condition is almost boundary lubrication on the vane side. At the theoretical analysis, μ_s is assumed to be constant and equal to 0.15.

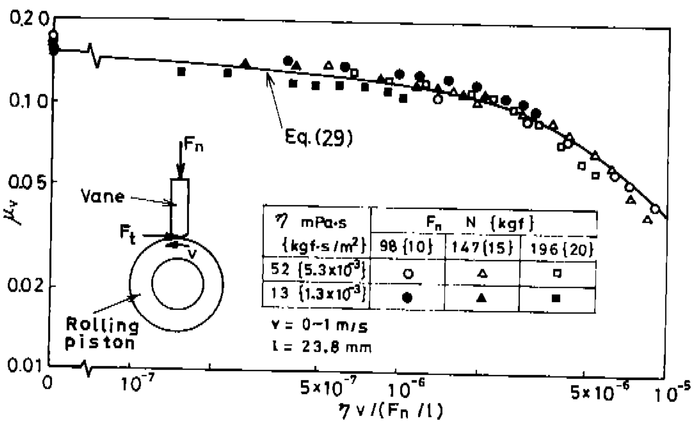

Fig. 10 Coefficient of friction at vane tip

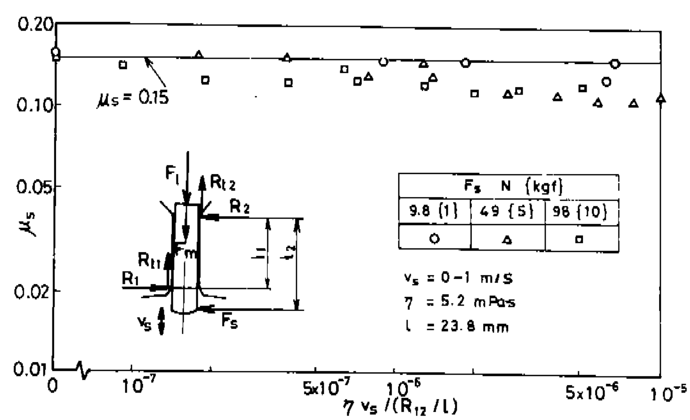

Fig. 11 Coefficient of friction at vane side

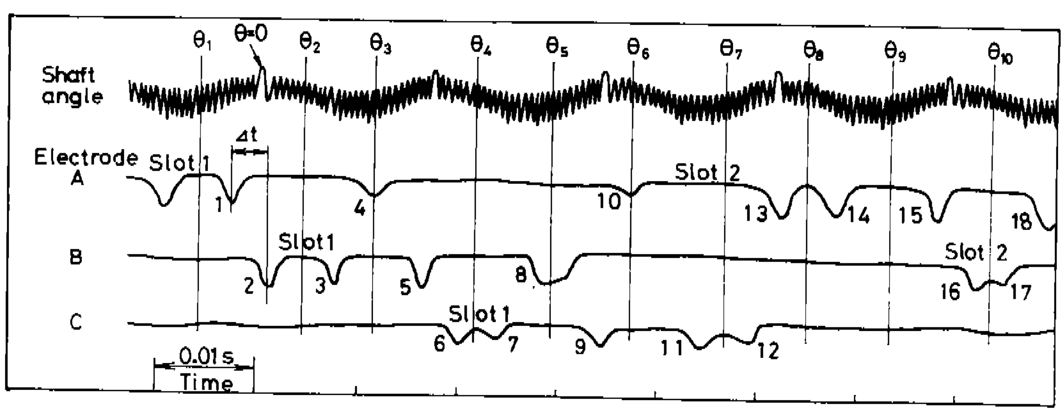

Fig. 12 Recorded chart of signals

Signal Analysis of Rolling Piston Motion

Figure 12 shows an example of recorded chart. It includes slot passing signals from three electrodes A, B and C. Downward peak of the signal means that a slot passes by the position of an electrode. Also, the signal of shaft angle is included in Fig.12. Larger upward peak of the signal indicates shaft angle $\theta=0$ rad.

Here, the location of rolling piston corresponding to $\theta=\theta_1$ in Fig.12 is assumed to be as shown in Fig. 13(1) and the slot locating just before the electrode A is named slot 1. In Fig.12, slot passing peaks 1 and 2 are recorded in the order of electrode A and B. This means slot 1 has moved to the position between electrodes B and C. The location of rolling piston at $\theta=\theta_2$ is considered to be as shown in Fig. 13(2). Then average velocity v_e of rolling piston at the place of electrodes is approximated by the next equation.

$$v_e = r_e \beta / \Delta t \tag{33}$$

Where, Δt is time difference between two peaks. Corresponding to v_e, angular velocity ω_p of rolling piston and sliding velocity v at vane tip are calculated as follows.

$$\omega_p = (v_e - e\omega \cos\theta) / (r_e - e \cos\theta) \tag{34}$$

$$v = r\omega_p + e\omega\cos\theta/\cos\alpha \tag{35}$$

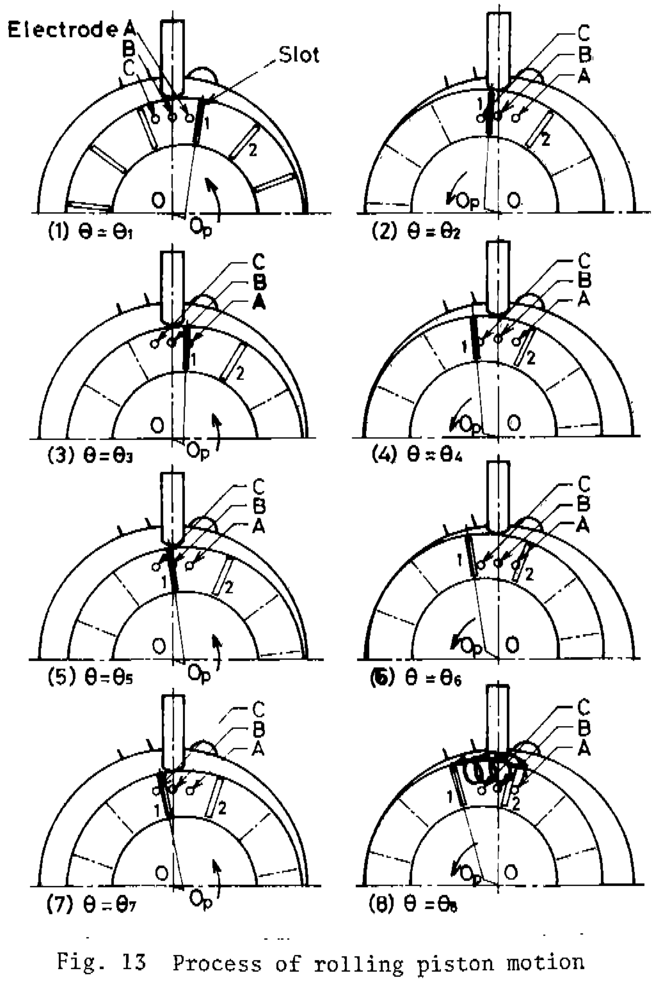

Fig. 13 Process of rolling piston motion

As slot passing peaks 3 and 4 are recorded in the order of electrodes B and A in Fig.12, rolling piston has moved backward during $\theta=\theta_2 \sim \theta_3$. Figure 13(3) shows location of rolling piston at $\theta=\theta_3$, just then slot 1 is overlapping with electrode A. Moreover, slot passing peaks 5 and 6 are recorded from electrodes B and C in Fig.12, which means slot 1 passes by position of electrode C as shown in Fig.13(4).

By analysis of signals shown in Fig.12 in the same manner, location of rolling piston corresponding to shaft angles $\theta=\theta_5 \sim \theta_8$ are decided as shown Fig. 13(5) ~ (8). Slot passing peaks 10, 13 ~ 15 and 18 from electrode A are contributed by the slot 2. In Fig.13(8), locus of fixed point to slot 1 on the rolling piston is drawn from $\theta=\theta_1$ to $\theta=\theta_8$. Rolling piston is revolving with its center and, as a whole, is rotating slowly around its center in the direction of shaft revolution.

Discussion of Results

Experimental and theoretical results of motion analysis of rolling piston will be discussed in the following. Theoretical results are obtained by nume-

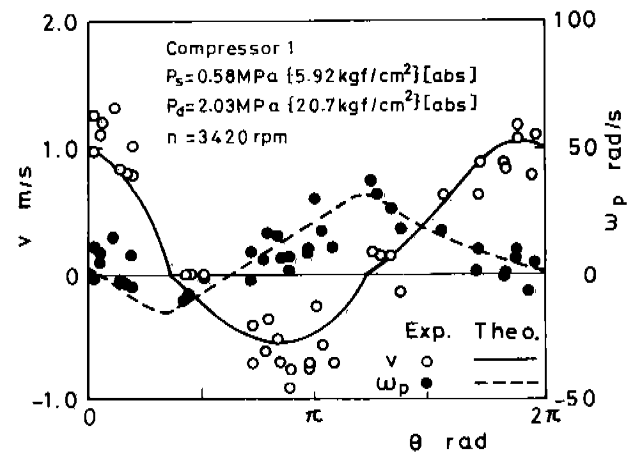

Fig. 14 Sliding velocity at vane tip and angular velocity of rolling piston (1)

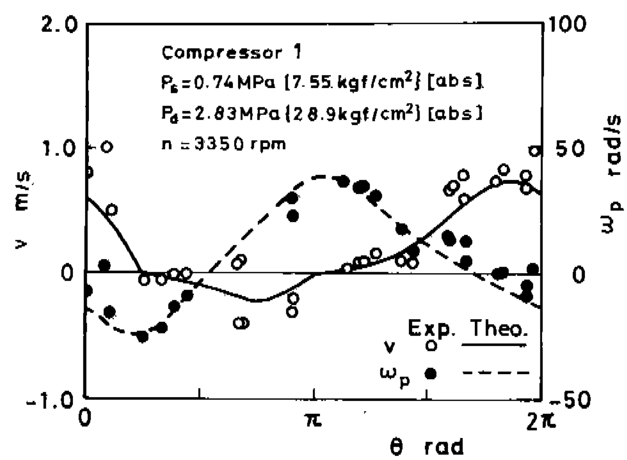

Fig. 15 Sliding velocity at vane tip and angular velocity of rolling piston (2)

rical calculation of Eqs.(1), (6), (7) using Runge-Kutta-Gill method. In that calculation, experimental coefficients of friction described before are used and viscosity of lubricating oil is rated taking account of solubility of refrigerant under operating pressure and temperature.

Figure 14 shows sliding velocity v at vane tip and angular velocity ω_p of rolling piston during one revolution of the shaft. v is positive in the neighbourhood of $\theta=0$ (2π) rad, which means rolling piston is sliding toward shaft revolution at vane tip. But in the neighbourhood of $\theta=\pi$ rad, v is negative, namely, rolling piston is sliding against shaft revolution.

On the other hand, ω_p is changing between positive and negative according to the change of v. But the maximum absolute value of ω_p is less than one tenth of shaft angular velocity (ω=360 rad/s). Therefore, at the right side of Eq.(35), the second term, which is sliding component based on revolving motion of rolling piston center around shaft center, is more influential on sliding velocity than the first term, which is the sliding component based on rotational motion of rolling piston around its center. In the neighbourhood of $\theta=\pi$, the second term becomes negative and v becomes negative, namely, backward sliding occurs at the vane tip.

Though experimental results shown in Fig.14 are a little scattered, they agree fairly well with theoretical results.

Figure 15 shows experimental and theoretical results when the compressor is operated with higher load than that in the case of Fig.14. Absolute value of v is less but amplitude of ω_p is larger as compared with those in Fig.14.

The decrease of sliding velocity means that, with increase of pressures, the increase of braking moment at vane tip is larger than the increase of driving moment at rolling piston bearing. In this case, theoretically calculated results are in good agreement with experimental results.

Table 2 shows list of average rotational frequency n_p of rolling piston for four designs of compressor under several operating conditions. As a whole, n_p is a few percentages of rotational frequency n of shaft. At the same compressor, n_p decreases with decrease of n and with increase of pressures. Under the same operating condition, n_p is different for each compressor design. As a whole, theoretical results agree fairly well with exprimental results.

Table 2 Comparison of experimental and theoretical results

Comp.	Operating condition			R. piston freq. n_p rpm	
	Pressur (abs.)		Freq.		
	p_s MPa	p_d MPa	n rpm	Exp.	Theo.
1	0.58	2.03	3420	64	77
	0.58	2.03	2880	62	56
	0.74	2.83	3350	63	54
2	0.58	2.03	3400	142	157
	0.58	2.03	2850	51	47
	0.72	2.53	3350	48	46
3	0.58	2.03	3450	132	131
	0.58	2.03	2880	49	67
4	0.58	2.03	3450	161	158
	0.58	2.03	2880	32	32
	0.72	2.53	3400	73	63

1 MPa = 10.2 kgf/cm^2

It is verified that theoretical calculation derived in this paper is valid to analyse rolling piston motion and to estimate the effects of operating parameter and design parameter of the compressor.

An Example of Friction Loss

Figure 16 shows an example of friction losses related to rolling piston motion and peculiar to this type compressor. Vane tip loss L_v, vane side loss L_s and rolling piston bearing loss L_c are derived from next equations.

$$L_v = v F_t \tag{36}$$

$$L_s = (R_{t1} + R_{t2})\dot{x} \tag{37}$$

$$L_c = \omega M_c \tag{38}$$

They can be easily calculated by using loss components resulted from motion analysis of rolling piston. Losses are waving during one revolution of the shaft affected by the rolling piston motion. In this case average of total loss L_t reaches about 7 % of average gas compression power of the compressor.

CONCLUSION

In this paper, motion of rolling piston in rotary compressor for air conditioner was analysed theoretically and experimentally.

It was proved that positive and negative sliding between vane tip and outer surface of rolling piston is occuring alternately during one revolution of shaft and rolling piston is rotating at average rotational frequency of a few percentages of shaft frequency. Rotational frequency of rolling piston decreased with decrease of shaft frequency and with increase of compressor load. Theoretical results using approximate theory of finite length bearing and empirical coefficients of friction agreed fairly well with experimental results and the validity of the theoretical analysis was verified.

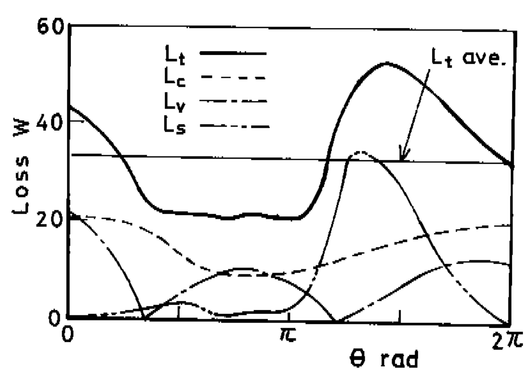

Fig. 16 Friction losses

NOMENCLATURE

a = vane length
a_1 = distance between vane tip and reaction point
b = vane thickness
c = radial clearance at rolling piston bearing
e = eccentricity of eccentric $=R-r$
F = bearing load
F_d = pressure differential force across vane within cylinder
F_e = centrifugal force of rolling piston
F_h = pressure differential force across vane in and out of cylinder
F_k = vane spring force
F_ℓ = force of cantilever
F_m = inertial force of vane
F_n, F_t = nomal and tangential force at vane tip
F_p = gas compression force of rolling piston
F_r, F_θ = radial and angular components of bearing load
F_s = force of spring balance
I_p = moment of inertia of rolling piston
L_c = friction loss at rolling piston bearing
L_s = friction loss at vane side
L_t = total friction loss $=L_c+L_s+L_v$
L_v = friction loss at vane tip
ℓ = cylinder length
ℓ_c = eccentric length (=bearing length)
ℓ_1, ℓ_2 = distances between force acting points
M_b = friction moment at rolling piston face
M_c = friction moment at rolling piston bearing
m_p = mass of rolling piston
m_v = mass of vane
n = rotational frequency of shaft
n_p = rotational frequency of rolling piston
p = pressure
p_b, p_c = pressures in suction and compression chambers
p_s, p_d = suction and discharge pressures of compressor
R = cylinder radius
R_{t1}, R_{t2} = tangential forces at vane side contact points
R_1, R_2 = nomal forces at vane side contact points
R_{12} = R_1+R_2
r = rolling piston outer radius
r_c = eccentric rarius (=bearing radius)
r_e = pitch circle radius of electrodes
r_v = vane tip radius
Δt = time difference between signals
V_c = compression chamber volume
V_s = suction volume
V_t = clearance volume
v = sliding velocity at vane tip
v_e = average velocity of slot
v_s = sliding velocity at vane side
x = vane extension $=R+r_v-(r+r_v)\cos\alpha-e\cos\theta$
x_0 = initial deflection of vane spring
z = coordinate of bearing length
α = offset angle of rolling piston center $=\mathrm{Sin}^{-1}\{e/(r+r_v)\times\sin\theta\}$
β = pich angle of electrode
δ_b = total clearance on rolling piston faces
ε = attitude of bearing
η = viscosity of lubricating oil
θ = rotational angle of shaft
θ_f = directional angle of bearing load
κ = adiabatic exponent
μ_s = coefficient of friction at vane side
μ_v = coefficient of friction at vane tip
ϕ = attitude angle of bearing
ψ = coordinate of bearing angle
ω = angular velocity of shaft
ω_p = angular verocity of rolling piston
$\cdot$ = time differential

REFERENCES

1 Okada,K., and Kuyama,K., "Analysis on Planetary Motion of the Rolling Piston in a Rotary Compressor (Theoretical Analysis of Mechanical Friction)," (in Japanese), Refrig., Japan. Vol.50 No.571, 1975. pp.331-337.

2 pandeya,P., and Soedel,W., "Rolling Piston Type Rotary Compressors with Special Attentions to Friction and Leakage," Proc. Purdue Compressor Tech. Conf., 1978, pp.209-218.

3 Chu,I., et al., "Analysis of the Rolling-Piston type Rotary Compressor," Proc. Purdue Compressor Tech. Conf., 1978, pp.219-224.

4 Ozu,M., and Itami,T., "Efficiency Analysis of Power Consumption in Small Hermetic Refrigeration Rotary Compressors," Int. J. Refrig., Vol.4 No.5, 1981, pp.265-270.

5 Nakagawa,E., and Aoki,H., "Dynamic Characteristics of Rotor - Bearing System Supported by Journal Bearings," (in Japanese), Lubrication, Japan, Vol.13 No.3, 1968, pp.117-125.

6 Nakagawa,E., and Aoki,H., "A Calculation Method of Characteristic Performance of Journal Bearings Under Dynamic Loading," (in Japanese), Lubrication, Japan, Vol.15 No.7, 1970, pp.385-390.